ARMA 18-1027

# Using the Energy Index Method to Evaluate Seismic Hazards in an Underground Narrow-Vein Metal Mine

Dehn, K.K.
*CDC NIOSH, Spokane, Washington, USA*

Butler, T.
*Engineering Seismology Group (ESG), Kingston, Ontario, Canada*

Weston, B.
*U.S. Silver-Idaho, Galena Mine, Wallace, Idaho, USA*



**ABSTRACT:** A routine method of evaluating temporal and spatial changes in relative rock mass stress levels based on microseismic information was developed by NIOSH researchers in collaboration with U.S. Silver Corporation's Galena Mine. The method is based on the Energy Index concept of Aswegen and Butler (1993), but was modified to evaluate the "running average" of inferred stress levels in a given seismogenic region for a selected time window. The new Average Scaled Energy Index method proved to be informative and efficient in providing daily information to mine operations personnel on the changing nature of stress in the rock mass due to mining and provided a standardized means to evaluate and compare conditions in different parts of the mine. It was found that underground mining crews easily understood the concept and adopted the method into daily operations. This paper discusses the initial evaluation and implementation of the modified method at the Galena Mine and provides three examples from different areas of the mine having distinct geologic and seismic characteristics to demonstrate its effectiveness.

## 1. INTRODUCTION

Mining-induced seismicity has been monitored almost continuously at the Galena Mine in the Coeur d'Alene mining district of Idaho, U.S.A., since 1968. Daily seismic hazard analyses of selected mining areas started in the late 1980s using multiple methods, including magnitude relationships, decay rates, and energy release rates. One of the difficulties experienced at the mine was the time required to complete the daily seismic analyses for each of the different mining areas due to their unique seismologic and geologic parameters, which required a high degree of familiarity by the ground control staff. The method was not sustainable under these conditions with both new ground control staff and mining crews lacking the requisite knowledge of the specific rock mass regions, particularly when they were moved into unfamiliar parts of the mine.

The Energy Index (EI) method, as developed by Aswegen and Butler (Aswegen and Butler, 1993) for use in the deep level South African gold mines, was recently evaluated as an alternative analysis method. The application of the EI method at the Galena Mine is a bit different than in previous studies because the mine no longer produces as many large events comparable to the deep South African gold mines, but the installed seismic array has very good coverage of the production areas which produce hundreds of small microseismic events daily. The objective of this study was to determine whether the EI method could be applied effectively to a catalog of small magnitude microseismic events and if the information would be as meaningful.

The initial evaluation included first identifying the appropriate volume constraints on areas of interest. Within each area, the seismic energy to seismic moment relationships were determined to calculate the EI values. A modification, referred to as the Average Scaled Energy Index (ASEI), provided a way to evaluate the running average of the seismicity in a given seismogenic region for a selected period of time, utilizing real-time data acquisition from the in-mine Engineering Seismology Group (ESG) seismic monitoring system. The results of the evaluation are presented in three examples from discrete volumes of the rock mass having distinct geologic and seismic characteristics.

## 2. BACKGROUND

### *2.1. Geological Setting*

The U.S. Silver Corporation's Galena mine is located in northern Idaho, U.S.A, in the Coeur d'Alene Mining District along the Silver Belt producing primarily silver and lead concentrates with some copper byproducts. The region is structurally complex and dominated by steeply dipping shear structures associated with the Lewis and Clark Line (White, 1998). Figure 1 gives a general location of the mine within the Coeur d'Alene mining district.

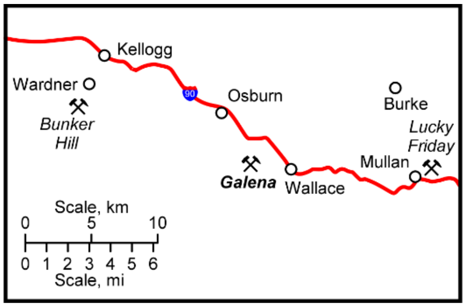


Fig. 1. Location of the Galena Mine in the Coeur d'Alene mining district.

The overall structure of the mine aligns with the major WNW striking faults in the area and associated shear structures between them as illustrated in Figure 2. Mineralized zones commonly occur as structurally controlled narrow veins along discrete sections of the faults and shear structures, primarily where they intersect with the steeply dipping metasedimentary Upper Revett Formation (Mauk and White, 2004). Veins are typically between 1.2–3 m in width. Zones of economically viable disseminated mineralization with widths up to 10 m have recently been identified. Due to the oblique orientation of the faults with the steeply upturned sedimentary units, the mine is approximately 1530 m along strike, with en-echelon mineralized zones spaced approximately 395 m apart. Mineralized zones can have vertical extents from 90–920 m.

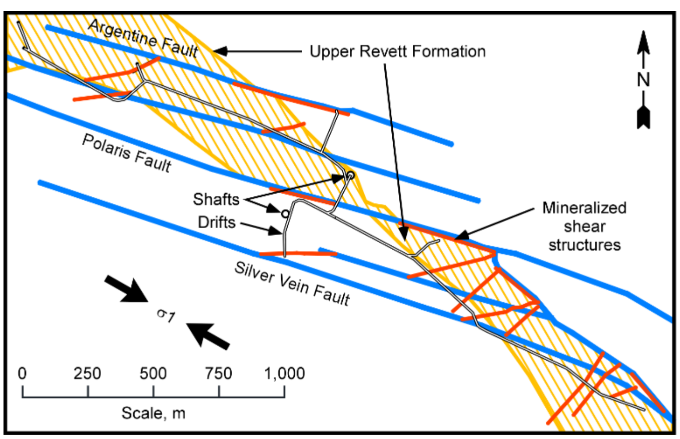


Fig. 2. Plan view of mine showing alignment with faults and Sigma 1.

Current mining occurs between 750 m and 1585 m below surface. The principal stress is oriented parallel to the WNW striking regional lineaments with magnitudes from 1.2–1.5 times the vertical overburden (Ageton, 1967). The combination of depth, high horizontal in-situ stress, and relatively strong wall rocks is conducive to mining-induced seismicity. Each of the mineralized zones across the mine tend to have unique seismogenic characteristics due to local wall rock assemblage and structural geometries. Figure 3 shows an example production area where seismic activity displays the linearity and clustering associated with structural control. Seismogenic volumes are generally defined by structural controls around the mining areas of interest.

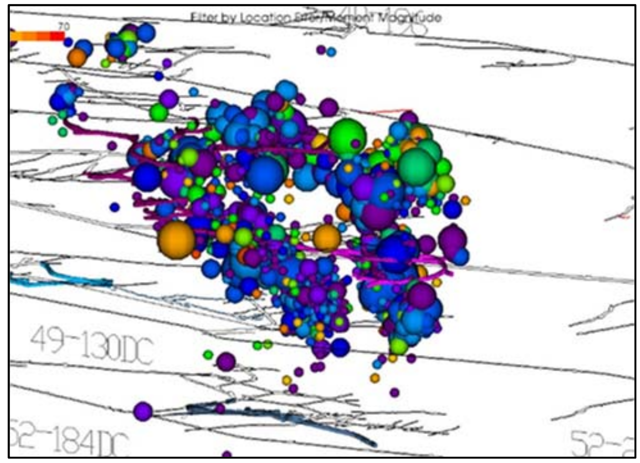


Fig. 3. Isometric view looking NW at one of the mining areas, showing tightly clustered seismic events along structures.

Mineralized zones typically have hydrothermal bleaching and silica flooding. Rock mass classification shows rock mass rating (RMR) values are normally from 25–70 driven primarily by moderate to strong fracturing and bedding plane detachments. Strengths vary from 77–225 MPa (Chan, 1971) and are strongly anisotropic due to bedding.

## 2.2. *Mining Methods*

Mining from the late 19th century to the early 1950s primarily utilized timbered cut-and-fill to depths up to 600 m with minimal backfill. Discovery of the Silver Vein on the 3000-level (914 m below surface) in 1953 and subsequent mining to greater depths encountered increased stress loads, resulting in increased dilution from overbreak and damaging mining-induced seismicity. To increase the ore grade and mitigate the seismic activity, the mine began using horizontal overhand cut-and-fill from captive timber raises, using hydraulic sand backfill (Visnes, 1957). Initially, this method resulted in continuous flat-backed mining fronts where stopes came up under crown pillars. Multiple damaging rockbursts resulted. Modification to stope sequencing was initiated in 1958 (Leisk, 1958), which reduced the number of rockbursts. Other modifications, such as de-stress blasting and the use of a modified vertical longwall, allowed extraction of many crown pillars, albeit with some large associated seismic events (Blake and Hedley, 2003).

Modification to the backfill infrastructure in 2000–2001 allowed for production of cemented hydraulic sand for underhand cut-and-fill (UCF) mining. Mechanized UCF allowed the recovery of a number of crown pillars in areas with high rockbursting potential (Williams et al., 2007). Seismic activity is still occurring, but the incidence of damaging rockburst events has decreased. Underhand mining has also provided flexibility to access small reserve blocks in areas below production levels where there is limited access from deeper levels.

### 2.3. *Seismic Monitoring System*

A seismic monitoring system has been in operation at the Galena Mine since 1968 (Blake and Leighton, 1971). Initially, seismic arrays were deployed around individual stopes with high rates of seismic activity. In 2002, an ESG seismic monitoring system replaced the aging seismic monitoring system installed by the U.S. Bureau of Mines (USBM) (Estey, 1995) and allowed real-time monitoring of the whole mine. Expansions to the system were completed in 2008 and 2012 to incorporate expanding mining fronts and improve detection in high-risk areas (Dehn and Knoll, 2013).

The current array has 50 sensors of which 35 sensors are repurposed 40 V/g Wilcoxon uniaxial accelerometers from the older USBM system. These are mixed with 14 x 30 V/g ESG uniaxial accelerometers and one 15-Hz ESG triaxial geophone. While not an ideal blend of sensor types, the system is able to detect and locate events down to moment magnitude (Mw) −2.5 with a location error of 10 m or less in the well-covered mining areas. Figure 4 is a schematic long section of the mine showing location of existing sensors.

An ESG strong ground motion system (SGM) runs in parallel with the microseismic system and provides source parameters for larger events. The SGM consists of three 4.5-Hz ESG triaxial geophones spaced approximately 1800 m apart; one installed in an adit near the surface and two underground at opposite ends of the mine.

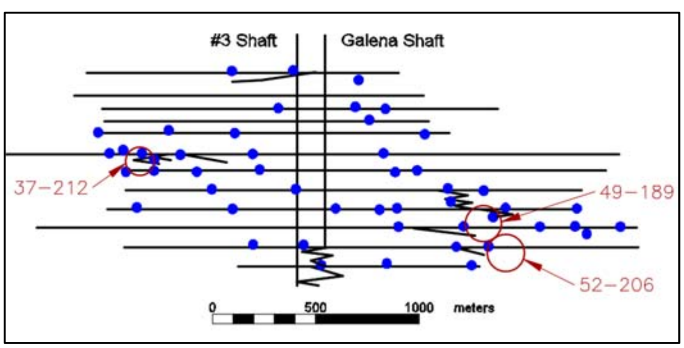


Fig. 4. Schematic long section of the Galena mine looking N35W, showing current location of sensors (blue dots). Areas of discussion from this paper are circled.

Mining-induced seismicity is a fact of life, and daily analyses of the seismic data is still required to ensure the rock mass is not negatively responding to changes in stress due to mining. Depletion of reserves close to the shafts has pushed the mining fronts laterally to the east and west following the discrete mineralized zones, increasing the number of production areas requiring individual evaluation. The result is an increased workload for the mine seismologist/ground control engineer. The amount of time spent evaluating each area of the mine on a daily basis was interfering with other important work at the mine. A more automated method to evaluate the nature of seismicity on a routine basis was required. A similar situation is discussed by Butler (Butler, 1997) at the Western Deep Levels Mine in South Africa that resulted in the development of the Weighted Energy Index concept. This method systematized a general interpretation of seismic data and presented the information in a format that was easily understood by mining personnel. These systematic reporting methods also reduce a mine’s reliance on any one individual for seismic data interpretation. This can be critical when specialist turnover happens at a mine, resulting in the loss of a wealth of site-specific knowledge and experience.

Methods of interpreting the nature of seismic data and stress state in the rock mass, such as the more traditional analysis methods of Gutenberg-Richter (G-R) relationships and Energy Release Rates (ERR), are difficult concepts to explain to operations personnel who may not have the necessary technical background to truly understand their meaning.

## 3. ENERGY INDEX METHOD

The Energy Index is a relative measure of energy release for a given amount of co-seismic deformation. The mine in this study worked with ESG to evaluate utilizing the EI method as a faster way to conduct daily and weekly analyses.

The method involves first determining the linear fit to a Log Energy (Log E) versus Log Seismic Moment (Log Mo) graph. The EI is then calculated as the ratio of the energy released per amount of seismic moment (co-seismic deformation) compared to the average for the volume and timeframe of interest. Within a given volume of the rock mass, an increase in the EI for seismic events over time generally indicates an increase in the relative stress levels, while a decrease in EI indicates a decrease in the relative stress levels. The method can also be used to compare relative stress levels between different rock mass volumes at a given point in time, which allows the ground control engineer to better evaluate the nature of rock mass response to mining and to prioritize action on areas that may not be deforming as expected based on numerical models or past experience.

### 3.1. Selection of Data for Energy Index Analysis

Not all seismic data recorded by the monitoring system should be used for the EI analyses due to limitations related to sensor types, coverage around a given volume, and magnitudes of the events. To remove the unwanted data, cut-offs were determined for each seismogenic volume during the quantile-quantile (Q-Q) comparison of the Log E and Log Mo for developing the EI relationship. The cut-off limits are unique to each seismogenic volume. In most areas, the lower limit was defined by the amount of sensors with good coverage of an area, and the upper limit was defined by the sensitivity of the sensor type.

Figure 5 below shows the unfiltered data for an individual seismogenic volume. Note the heavy tail (left) and data scatter (right) at the ends of the line where the data quality for events is becoming compromised due to the upper and lower detection limits of the seismic array. For the array in use at the mine, the lower detection limit indicates where there is a low signal to noise ratio and/or to too few sensors in a location solution, leading to suspect source parameter calculations. The upper limit is related to predominant use of high-frequency accelerometers where source parameters for larger events are suspect due to a lack of geophones. Data falling outside the cut-offs are excluded from the EI line fitting.

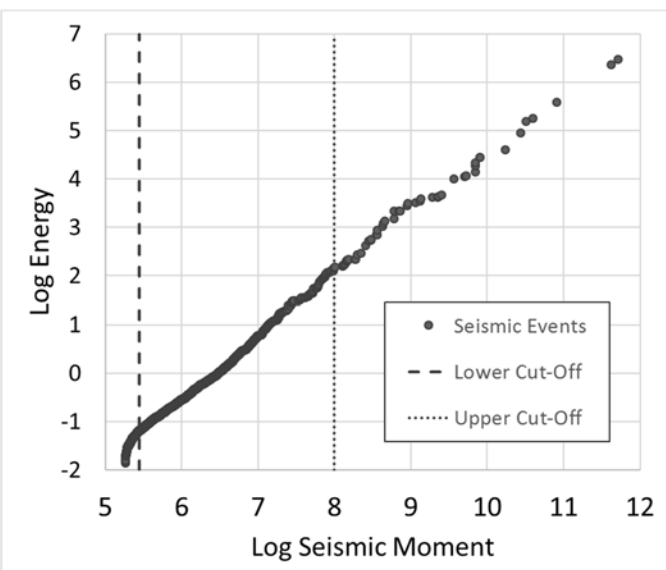


Fig. 5. QQ Plot of all seismic data within a seismogenic volume (N=2609). Note the heavy tail at the lower values and the scatter at the upper Seismic Moment values.

### 3.2. Average Scaled Energy Index

In practice, the EI was converted to a Scaled Energy Index (SEI), which is a variation of EI that results in values that are numerically scaled equally above and below the average. The equations are shown in Equation 1 and 2.

$$\text{For EI} > 1 \qquad \text{SEI} = \text{EI}-1 \tag{1}$$

$$\text{For EI} < 1 \qquad \text{SEI} = -(1/\text{EI})+1 \tag{2}$$

An SEI greater than 0.0 means that there is more energy released than the average and is interpreted as indicating a higher stress event. An SEI < 0.0 means that there is less energy released for the event than the average. A plot of the SEI values for a given volume over time is shown in Figure 6.

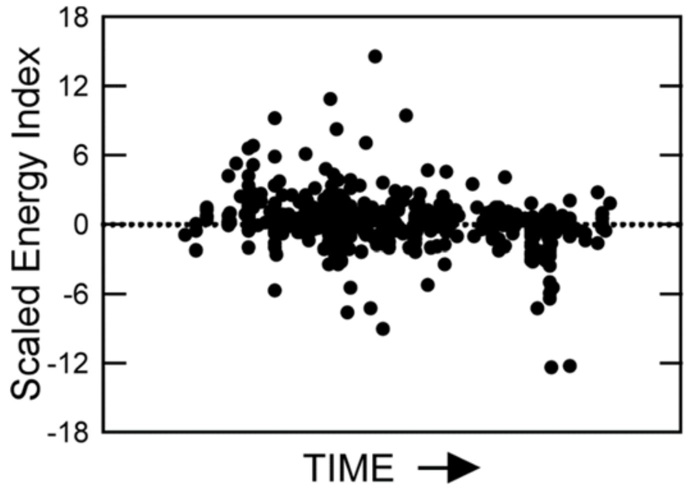


Fig. 6. SEI values from a volume of interest. Note the spread above and below the dotted zero line indicating the average EI.

To capture the overall trends, the SEI values were averaged over a moving window of time to create the Average Scaled Energy Index (ASEI) values. Varying time windows were tested to determine which of the windows proved to be most informative. Time windows of 24 hours, 72 hours, 7 days, and 28 days were the most useful, but were highly dependent on the amount of data points available for the volume of interest. Where data points are widely spaced in time, a short time window creates a highly variable trend line, heavily influenced by individual events. Such an erratic line may cause an inaccurate assessment of the stress trends for the area.

Figure 7 shows the moving average of the ASEI along a fault line over a period of 5 months. The 24-hour line is very erratic, though for the total length of time observed, an increase and decrease in the overall ASEI values is notable. The 7-day line nicely smooths out the data while still responding to daily or multi-day changes such as blasting or mining.

In areas with active daily blasting and moderate seismic rates of 1–3 events per hour, a 72-hour time window corresponded well to blasting and anticipated stress changes. In areas with 3–5 events/hour or more, a 24-hour window can be informative. In areas of low activity with event rates closer to 1–3 events per day or less, a time window of 28 days was useful. With the larger time window, the trend lines lagged significantly behind daily or weekly activities, such as blasting, and are not recommended for day-to-day analyses where decisions would have an effect on daily production.

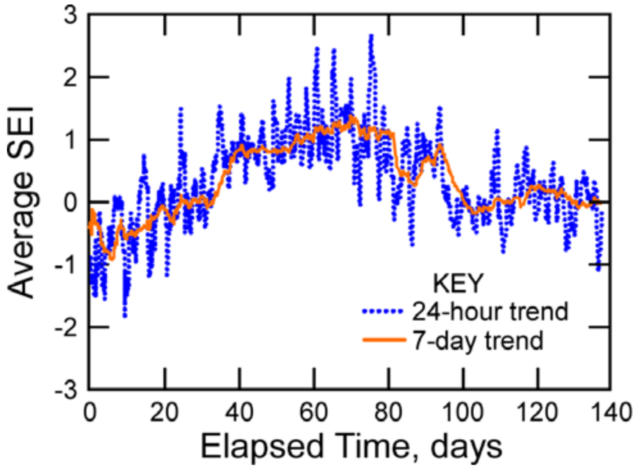


Fig. 7. Smoothing effects of time windows on the Average Scaled Energy Index (ASEI).

## 4. AREAS OF APPLICATION

The following case studies discuss three areas of the mine where the ASEI method was applied. The studies provide examples of how the ASEI method can be utilized in multiple ways and in varying seismogenic volumes to analyze the response of the rock mass to mining. Each of these areas are seismogenically unique, involving different structures as well as mining methods. The first example describes the use of the ASEI methods along a fault structure located on the east side of the mine with a very high extraction ratio. The second area examined is an active production area near the lower east side of the mine with minimal historical mining. The third area examined is a remnant pillar in the far west side of the mine, approximately 1525 m removed from the first two examples, located on completely separate geologic structures. Figure 4 shows the areas of application discussed, and they are circled for reference.

### 4.1. *The 49-189 Abandoned Sill Prep Collapse – Silver Vein Fault*

In August 2016, the 49-189 timber sill prep in an abandoned section of the mine collapsed due to perpendicular squeeze caused by fault movement. A schematic of the location is presented in Figure 8. Figure 9 shows a cross section of the timber prep. The seismic system recorded the collapse, and a review of the continuous seismic data feed confirmed that the failure did not result from an individual seismic event, such as a rockburst. The ESG system allows for audio output from individual channels. An accelerometer, located 254 m away, recorded cracking of the timber moments prior to failure. Failure of the sill prep allowed release of the hydraulic sand backfill contained above the prep. The sudden removal of confinement material (timber prep and the backfill material) allowed deformation of the rock mass into the open void. This deformation was recorded by the seismic system with a large increase in low-magnitude seismic activity around the stope.

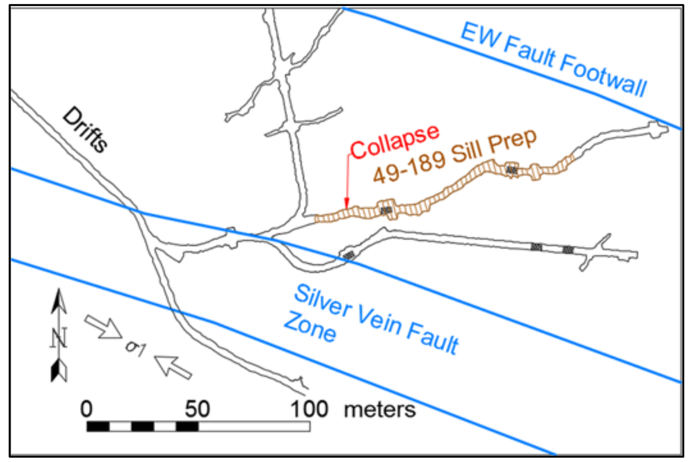


Fig. 8. Plan view of the 49-189 timber sill prep area that collapsed in August 2016. Major geological structures and maximum principle stress in the area are also shown. Drifts adjacent to the timber prep were not affected.

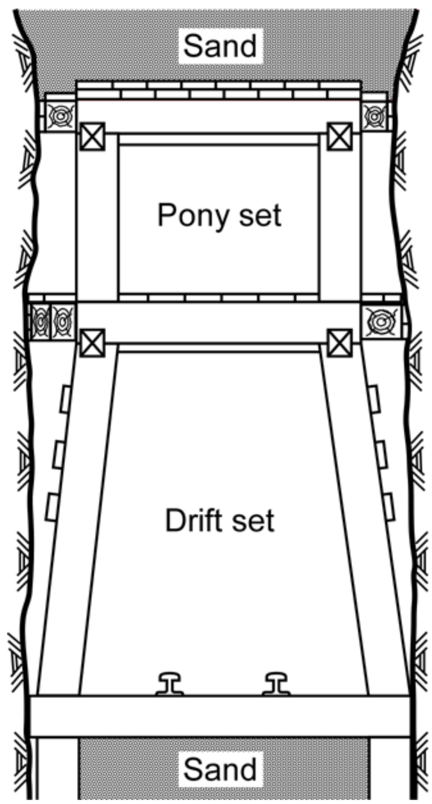


Fig. 9. Sectional view of a sill timber prep. The collapse occurred by buckling of the horizontal members in the Pony and Drift sets. (Modified after Staley, 1962).

The sill prep was located along a NE striking vein, oriented perpendicular to the maximum stress. The vein splayed off the larger EW striking Silver Vein Fault and connected to a second parallel EW fault deeper in the footwall. The NE vein had been entirely mined out between both faults over 430 vertical meters.

The area around the stope had produced small magnitude seismic activity consistently, mainly along the Silver Vein Fault to the south. Seismic event rates were normally around five events per day, even though mining in the area ceased in the late 2000s. Squeezing of the timber prep had been observed for a number of years prior to the failure.

Following the collapse, seismic event rates spiked up to 20–70 events per day for a week before settling to background levels. A back analysis of seismic data prior to the collapse examined daily seismic event rates, magnitude distributions, and other source parameters, but no unusual activity was indicated. The ASEI analysis identified an increase in relative stress levels, which started after cessation of mining along the Silver Vein Fault in September 2014. ASEI values were significantly lower than average while mining was occurring along the fault. Values began increasing immediately after cessation of mining, stabilizing after approximately three months. Values dropped slightly when a new mining area, located 300 m to the North along a parallel fault structure, began in May 2015 (approximately 360 elapsed days in Figure 10). Figure 10 shows the results of the average ASEI values from May 2014 to December 2016.

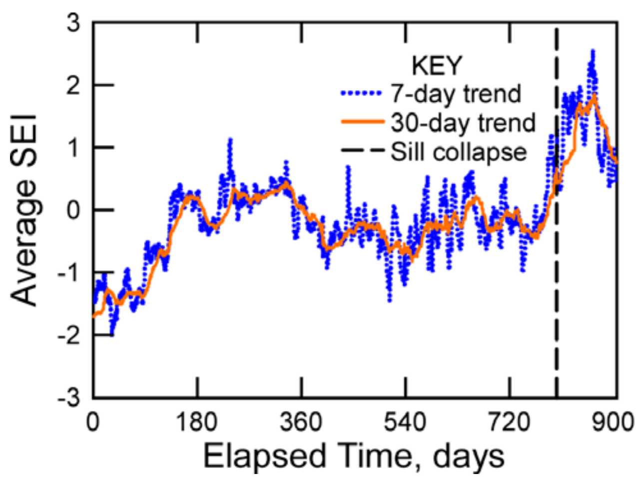


Fig. 10. Average Seismic Index along the Ag Vein Fault from May 2014 to December 2016 (900 days total).

A sudden increase in the ASEI began in early July of 2016 and could not be correlated to current mining activities in the area. The sill prep collapse occurred approximately one month later. The ASEI continued to climb for another month before leveling off and then declining. As of December 2016, the area had not returned to pre-collapse values.

Access to the 49-189 timber prep had been closed off a year prior to the collapse, so there was no way to inspect the area for any visible deformation in the months leading up to the collapse. The other accessible drifts closest to the collapse area did not show any signs of abnormal deformation. The change in the ASEI values was the only available indicator of a potential change in the area. Utilizing proximal microseismic data to observe the rock mass response to a static ground support failure could be a useful tool for monitoring other timber stope preps in similar orientations.

### *4.2. The 52-206 Pillar Yielding from a Rockburst*

A captive pillar was removed using mechanized UCF mining in early 2016. The stope was located along a bedding parallel fault structure, subparallel to the maximum stress. The footwall consisted of a soft, highly foliated argillite; the hanging wall consisted of a robust, thickly bedded quartzite. Small to moderate magnitude seismic activity was common primarily in the hanging wall, and to a lesser extent, in the footwall. Two crossing NS vertical fault structures, one at each end of the stope, controlled the lateral extent of seismicity and ore distribution. Figure 11 provides a schematic plan view of the area; the pillar is located along the 207 Pb Vein.

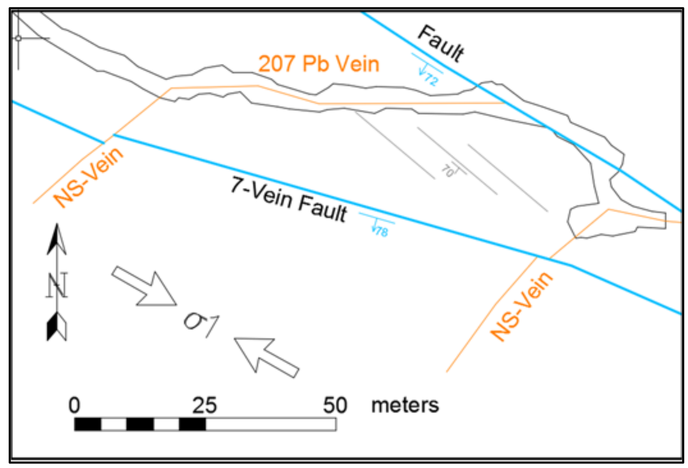


Fig. 11. Schematic plan view of the 52-206 stope, showing drifts, relevant geological structures, and maximum principal stress direction.

Daily analyses using the ASEI method were carried out using 24-hour and 72-hour time windows. Trend lines of the seismic data corresponded well to advancing excavations crossing the N-S structures and minor changes in azimuths of the cut. A Mw 1.4 rockburst, located approximately 10 m south in the hanging wall, occurred on March 5, 2016 during blasting. The seismic event resulted in moderate damage along the hanging wall close to the hypocenter, consisting of bagged mesh and fracturing of the cemented backfill above, but there was no major damage. Production was halted for a few days to repair the ground support and to reinforce the damaged backfill. When production resumed, daily seismic analyses indicated that the overall ASEI values had reduced to below average, indicating a stress reduction. Figure 12 shows the 24-hour and 72-hour trends before and after the event.

The drop in ASEI values required a re-evaluation of the Log E/Log Mo relationship for events after the burst. The results of the new comparison are shown in Figure 13. There is a distinct downshift between the two lines, indicating that seismic events were now producing lower energy values for similar seismic moment values. This was a reassuring indication that the burst had damaged the adjacent rock mass enough to allow de-stressing of the area.

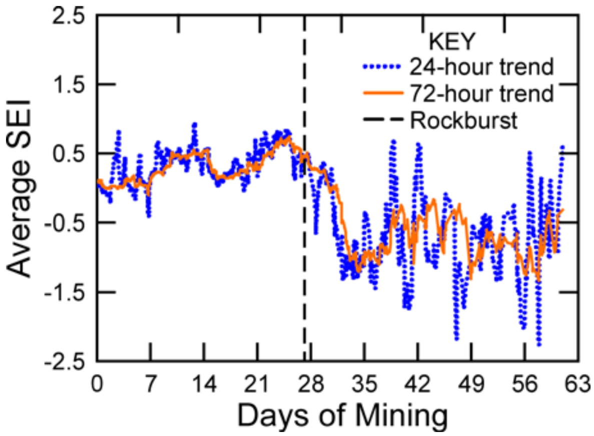


Fig. 12. The 24-hour and 72-hour SEI trends of the 52-206 stope prior to and after a large rockburst.

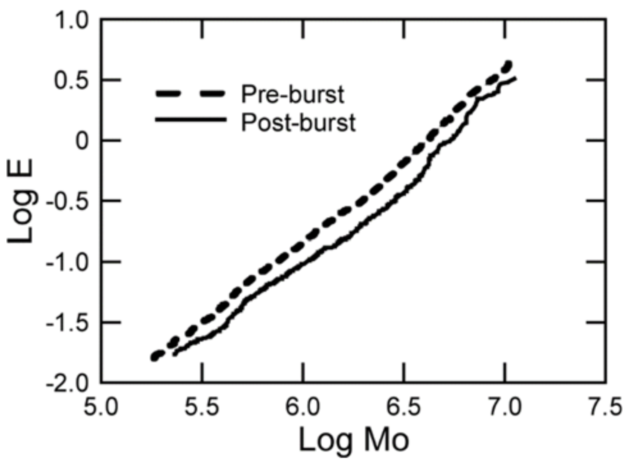


Fig. 13. A QQ comparison of Log E versus Log Mo values for seismic events before and after the March 5, 2016 rockburst in the 52-206 stope.

The re-evaluation was not necessary to continue using the ASEI method in the area; it was completed to help highlight any subsequent increases in the ASEI during future mining that might be a prelude to another rockburst. Mining of subsequent cuts confirmed that the rock mass appeared to be de-stressed as the new ASEI values remained lower than values from the previous cuts and no other large seismic events occurred. Full extraction of the pillar was achieved without further incidents.

### *4.3. The 37-212 Pillar Recovery*

Starting in 2015, a remnant pillar approximately 20 m in vertical height was extracted using mechanized UCF. The pillar was located along a steeply dipping high-grade vein structure with two distinct parts; the first half (east side) was along an EW fault structure, and the second (west side) turned along an intersecting NNE striking fault. The vein terminated against a crossing bedding parallel fault. Previous mining using conventional and mechanized methods had left the pillar open to the west, with full extraction along the top, base, and east side. Figure 14 provides a schematic plan view of the area surrounding the 37-212 stope.

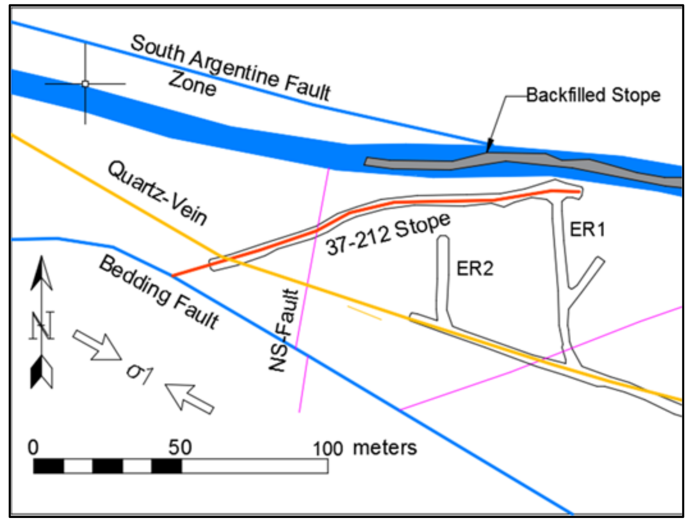


Fig. 14. Plan view of major structures and orientation of the 37-212 stope.

The area was historically very seismically active, producing a number of large, damaging rockbursts, up to Mw 3.0 associated with multiple faults in the area. A high extraction ratio from historical mining also produced zones of increased stress in remnant pillars. Because of the high seismic hazard, a detailed mine plan was developed utilizing numerical modeling and industry guidelines for mining in high-stress ground to manage the rockburst hazard and reduce the potential for damaging events. The plan initially required seven cuts for full extraction. The first four cuts would be mined “one sided,” meaning they started from an entry ramp (ER1) on the east side of the pillar, adjacent to backfill, and proceeded west across the top of the pillar below the cemented hydraulic fill. Numerical modeling indicated that peak induced stress loads would occur during cuts 3 or 4 and then decrease with subsequent cuts. Data from the seismic monitoring system would be analyzed to observe the performance of the pillar. Interpretation of the data would assist in deciding when the pillar load had decreased enough to safely excavate Cuts 5–7 from a second entry ramp (ER2) to be driven closer to the center of the pillar.

Initial mining of Cuts 1–3 did not encounter significant amounts of seismic activity until the face turned onto the NNE section of the stope. Event rates, magnitudes, and the ASEI trends increased at this point and remained elevated until the end of the cuts. This pattern was repeated for all subsequent cuts. Moderate to large seismic events began with Cut 3. Some seismic events were located within the pillar, and others occurred along nearby faults. Figure 15 shows the ASEI trends while mining along the NNE section of the stope during Cut 2.

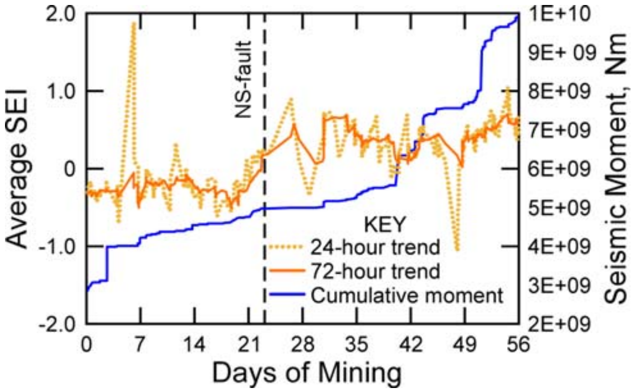


Fig. 15. The 37-212 Cut 2 24-hour and 72-hour ASEI trends for the NNE section of the vein.

An unexpected zone of high stress was encountered approximately 33 m from the end of the cut where the vein crossed a NS striking silicified fault. The intersection of this fault is identified in the data by the increase in the ASEI trends above average and is labeled in Figure 15 and 17. The cumulative seismic moment is plotted along with the trends and shows a relatively uniform slope until an exponential increase as the face approached within 20 m of the pillar edge.

Figure 16 compares the 72-hour ASEI trends along the NNE section of the vein for Cuts 2–5. The horizontal axis is the normalized number of mining days in the stope to allow a side-by-side comparison of the data. Cut 4 had the highest ASEI trend, the details for which are shown in Figure 17. The increased ASEI values during Cut 4 correspond well to the numerical modeling, which indicated a peak induced pillar load during Cut 3 or 4. The results from Cut 5 were initially erratic when ER2 first intersected the NNE section of the stope, after which ASEI values remained lower than during Cut 4. This was encouraging and interpreted as an indication that the central portion of the pillar had yielded. ASEI values near the end of Cut 5 were slightly higher than Cut 4, and this is interpreted as increased induced loading at the edge of the pillar.

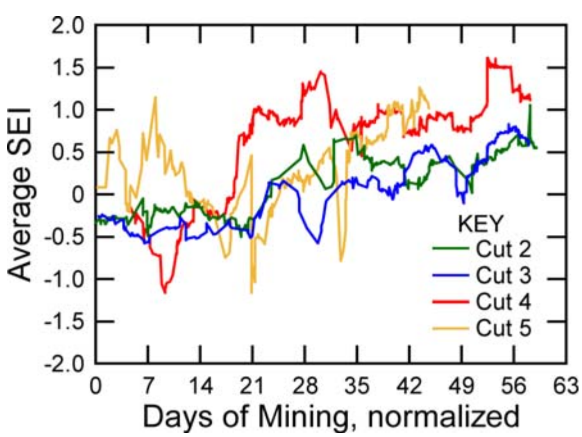


Fig. 16. Comparison of the SEI Values with time for Cuts 2–5 across the NNE section of the stope.

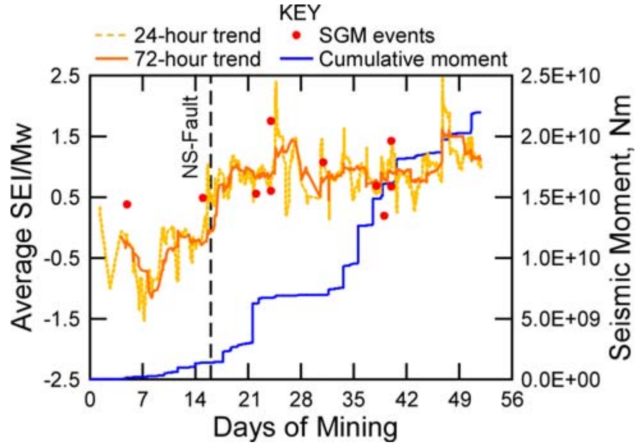


Fig. 17. Details of Cut 4. Dots represent moderate to large seismic events scaled by their moment magnitude (Mw) and plotted on the left vertical axis at the same scale as the ASEI.

Near the end of mining during Cut 4, the ASEI was used to indicate when crews should be pulled from the stope due to an increased seismic hazard. Underground crews in the 37-212 stope on day-shift reported that seismic activity was closer and louder than normal while drilling at the face near mid-day. Review of the seismic data showed that the area was experiencing an increase of the 24-hour ASEI trend, which was unusual for that time of day. Based on a review of data from the previous cuts, an increasing 24-hour ASEI trend had the potential for a moderate to large seismic event to occur with continued mining activity, such as drilling or blasting. The increased trend and its potential outcome was explained to the supervisors, and with their agreement, crews were immediately pulled from the stope and the area was barricaded until the next morning.

The following morning showed the 24-hour ASEI trend decreasing with no moderate or large events recorded in the area. Crews were allowed to return to the stope to finish drilling and loading the round. No adverse seismic activity occurred during this time. The round was blasted at the end of the shift, and a Mw 1.4 seismic event occurred with the blast causing minor damage near the face.

The success of using the method as a forecasting tool to pull crews where real-time data seemed to indicate that the area was becoming unstable was fortunate and encouraging. Use of the method as a forecasting tool requires a great deal more research, and in all likelihood, will be dependent on the level of experience and understanding a mine seismologist has with a seismogenic volume.

## 5. DISCUSSION

The initial evaluation of using the EI method at the Galena Mine, with some modification to produce ASEI values, proved to be applicable to the steeply dipping narrow vein ore bodies that are characteristic of the Coeur d'Alene district. The method provided an effective way to systematize the daily seismic analyses between mining areas that have different seismogenic characteristics. ESG has incorporated the EI method with the ASEI modifications into their SeisVis™ software (ESG Solutions, 2017) making it easier to teach new mine staff how to conduct the daily analysis.

In practice, ASEI values for individual events can be "spiky" in nature. Averaging the data over a moving window of time helps smooth out the scatter and can illuminate trends in the relative stress levels. The size of an appropriate time window is dependent on the number of data points available. The optimum time window size should be selected based on the amount of data available in the area/time of interest. Shorter time windows require sufficient data so that overall trends in ASEI values can be identified. Longer time windows should not be used for day-to-day planning, but are useful for identifying long-term trends in the relative stress levels.

The ASEI values can be utilized in multiple ways and in varying seismogenic volumes to analyze the response of the rock mass to mining. The three examples discussed successfully utilized the ASEI values to examine relative stress conditions around a fault and in two yielding pillars. The ASEI provided feedback that helped verify numerical modelling results adding some confidence the models adequately represent reality. The EI method can also be combined with other methods of seismic hazard analysis, such as magnitude distribution or cumulative moment, for improved insight as to how a seismogenic volume is behaving.

The EI method can be used successfully with seismic monitoring systems that may have suboptimal mixtures of sensors. All three examples discussed had excellent three-dimensional coverage by numerous sensors, though most of the sensors were surface-mounted uniaxial accelerometers, which is not an optimal installation. An array with mixed sensor types and improved down-hole installations would provide improved source parameters over a larger magnitude range, likely providing more interesting insights into the rock mass response, such as source mechanisms.

## 6. FUTURE WORK

Research is currently being conducted with ESG and NIOSH to utilize the EI method for comparison to concurrently collected instrumentation data to evaluate correlations in the physical rock mass response to mining/seismic activity and to develop improved methods of evaluating seismic hazards.

## 7. ACKNOWLEGEMENTS

The authors wish to thank U.S. Silver Idaho, Inc. and the Galena Mine for allowing the publication of this work. We would also like to thank ESG for all the advice and assistance in understanding and applying the Energy Index method.

## 8. DISCLAIMER



## REFERENCES

1. Ageton, R.W. 1967. Stress ellipsoid determination in a rock-burst-prone area at A 4,000-foot Depth, Galena Mine, Wallace, Idaho. U.S. Dept. of the interior, Bureau of Mines, RI 6997, 23 pp.

2. Aswegen, G.V. and A.G. Butler. 1993. Applications of quantitative seismology in South African gold mines, In *Proceedings of the 3rd International Symposium on Rockbursts and Seismicity in Mines, Kingston, Ontario, Canada, 16-18 August, 1993*, ed. R.P. Young, pp. 261–266. Rotterdam: Balkema.

3. Blake, W. and F. Leighton. 1971. Rock Burst Research at the Galena Mine, Wallace, Idaho. U.S. Bureau of Mines, TPR 39, 22 pp.

4. Blake, W. and D.G.G. Hedley. 2003. Galena Mine – Wallace, Idaho. In *Rockbursts: Case Studies from North American Hard-Rock Mines*, Littleton, Colorado, Society for Mining, Metallurgy, and Exploration, Inc.

5. Butler, A.G. 1997. Application of weighted energy index for routine evaluation of rockburst potential. In *Proceedings of the 4th International Symposium on Rockbursts and Seismicity in Mines, Krakow, Poland, 11-14 August, 1997*, eds. Gibowicz, S.J., Lasocki, S., pp. 317–323.

6. Chan, S.S.M. 1971. Deformation behaviour of Revett Quartzite under uniaxial and triaxial Loading. In *Proceedings of the 6th Canadian Rock Mechanics Symposium, Montreal, May 1970*, Publication Mines Branch – Dept. of Energy, Mines and Resources, Ottawa, pp. 9–31.

7. Dehn, K., and S. Knoll. 2013. Expansion, Performance, and Improvement of the Rock Burst Monitoring System at the Coeur, Galena and Caladay Mines, Wallace, ID. In *Proceedings of the 47th U.S. Rock Mechanics/Geomechanics Symposium, San Francisco, California, 23-26 June, 2013*, Paper #281.

8. ESG Solutions. 2017. Seismic Visualizer Brochure. Available from ESG Solutions at ESG website https://www.esgsolutions.com/contact.

9. Estey, L.H. 1995. Overview of USBM microseismic instrumentation and research for rock-burst mitigation at the Galena Mine, 1987–1993. In

*Proceedings: Mechanics and Mitigation of Violent Failure in Coal and Hard-Rock Mines,* USBM Special Publication 01-95, eds. H. Maleki, et al., pp. 283–302.

10. Leisk, R.D. 1958. Report on the rock burst conditions at the Galena Mine as of July 31, 1958. Internal report, American Smelting and Refining Company.
11. Mauk, J.L., and B.G. White. 2004. Stratigraphy of the Proterozoic Revett Formation and its control on Ag-Pb-Zn Vein Mineralization in the Coeur d'Alene District, Idaho. *Economic Geology*, Vol. 99, pp. 295–312.
12. Staley, W.W. 1962. Timbering and support of underground workings for small mines. *Idaho Bureau of Mines and Geology, Bulletin No. 21,* Moscow, Idaho, Figure 7.
13. Visnes, N. 1957. Sand filling at the Galena Mine. In *Mining Engineering*, January. In *The American Institute of Mining, Metallurgical, and Petroleum Engineers,* pp. 49–52.
14. White, B.G. 1998. New tricks for an old elephant: Revising concepts of Coeur d'Alene geology. *Mining Engineering,* August, pp. 27–35.
15. Williams, T., T. Brady, D. Bayer, M. Bren, R. Pakalnis, J. Marjerison, and R. Langston. 2007. Underhand cut and fill mining as practiced in the three deep hard rock mines in the United States. In *Proceedings of the 109$^{th}$ CIM AGM, Montreal, Quebec, Canada, April 29–May 2, 2007*, 11 pp.